J. Fluid Mech. (2002), *vol.* 459, *pp.* 103–128.
DOI: 10.1017/S0022112002007899 Printed in the United Kingdom

Lubrication theory for electro-osmotic flow in a microfluidic channel of slowly varying cross-section and wall charge

By SANDIP GHOSAL

Department of Mechanical Engineering, Northwestern University, 2145 Sheridan Road, Evanston, IL 60208, USA

(Received 24 August and in revised form 2 November 2001)

Electro-osmotic flow is a convenient mechanism for transporting fluid in microfluidic devices. The flow is generated through the application of an external electric field that acts on the free charges that exist in a thin Debye layer at the channel walls. The charge on the wall is due to the particular chemistry of the solid–fluid interface and can vary along the channel either by design or because of various unavoidable inhomogeneities of the wall material or because of contamination of the wall by chemicals contained in the fluid stream. The channel cross-section could also vary in shape and area. The effect of such variability on the flow through microfluidic channels is of interest in the design of devices that use electro-osmotic flow. The problem of electro-osmotic flow in a straight microfluidic channel of arbitrary cross-sectional geometry and distribution of wall charge is solved in the lubrication approximation, which is justified when the characteristic length scales for axial variation of the wall charge and cross-section are both large compared to a characteristic width of the channel. It is thereby shown that the volume flux of fluid through such a microchannel is a linear function of the applied pressure drop and electric potential drop across it, the coefficients of which may be calculated explicitly in terms of the geometry and charge distribution on the wall. These coefficients characterize the 'fluidic resistance' of each segment of a microfluidic network in analogy to the electrical 'resistance' in a microelectronic circuit. A consequence of the axial variation in channel properties is the appearance of an induced pressure gradient and an associated secondary flow that leads to increased Taylor dispersion limiting the resolution of electrophoretic separations. The lubrication theory presented here offers a simple way of calculating the distortion of the flow profile in general geometries and could be useful in studies of dispersion induced by inhomogeneities in microfluidic channels.

1. Introduction

Many solid substrates, (such as glass, silicon, polymeric materials, minerals) acquire a surface charge when in contact with electrolytes. The charged surface attracts free ions of the opposite sign creating a thin ($\sim$ 1–10 nm) Debye layer of mobile charges next to it. In the presence of an external electric field, the fluid in this Debye layer acquires a momentum which is then transmitted to adjacent layers of fluid through the effect of viscosity. The resulting fluid motion is known as electro-osmotic flow (Probstein 1994). Since the force per unit length of channel is proportional to the circumference of the channel while the mass of fluid that must be moved is proportional to the cross-sectional area, the effect is significant in very narrow channels

such as those etched on substrates ($\sim$ 10–100 μm diameter or less) in microfluidic devices, or, in the interparticle spaces in porous media. Electro-osmotic flow was first reported by Reuss in 1809 in experiments that demonstrated that water could be made to percolate through porous clay diaphragms through the application of an electric field (Reuss 1809).

In recent years, electro-osmotic flow (EOF) has found wide application in microfluidic devices as an efficient method for transporting fluid (Jakeway, de Mello & Russell 2000; Whitesides & Stroock 2000). The convenience of being able to move fluid by applying voltages along the channels, has the advantage that electric and fluidic circuits can be integrated on the same microchip to build complex miniaturized devices without moving parts. In addition, EOFs in uniform channels have a constant velocity over the channel cross-section (except within the thin Debye layer at the wall). This is in contrast to the situation in pressure-driven flows, such as the Poiseuille flow in circular pipes, where the velocity distribution has a parabolic profile. As a result, in EOF Taylor dispersion (Probstein 1994) of solutes is very small. This is a great advantage in many bioanalytical applications of microfluidics. For example, the resolution in electrophoretic separation of biomolecules of only slightly differing mobilities is limited by Taylor dispersion (Culbertson, Jacobson & Ramsey 1998).

The uniformity of the flow profile and the resulting low Taylor dispersion are characteristic of microfluidic channels with a uniform wall charge. In the presence of inhomogeneities in the wall charge, induced pressure gradients are created that distort the uniformity of the flow profile (Herr *et al.* 2000), reducing the efficiency of microfluidic devices that use EOF for electrophoretic separations. A common cause of non-uniformity of the wall charge is the adsorption of certain organic molecules onto the wall during analysis (Towns & Regnier 1991, 1992). Further, the wall charge depends strongly on the pH of the buffer and is known to exhibit hysterisis effects when the pH is changed (Lambert & Middleton 1990). Various synthetic materials such as acrylic and Poly(dimethylsiloxane) (PDMS) are being investigated as possible replacements for glass or silicon substrates on account of their lower cost among other advantages (Anderson *et al.* 2000). A difficulty with the use of such materials is that the wall charge is not as uniform as in the glass and silicon-based devices. In order to overcome such difficulties and allow more precise control over the wall charge, various synthetic coatings are being investigated (Liu *et al.* 2000). With such techniques, channels with a specified variation of the wall charge could be engineered to build novel fluidic properties into micro devices (Barkar *et al.* 2000). Control of wall charge using externally applied voltages has also been studied (Lee, Blanchard & Wu 1990; Hayes & Ewing 1992).

In light of these continuing developments in microfluidic technology, the problem of EOF in microfluidic channels of variable wall charge is of great interest. Anderson & Idol (1985) considered the problem of EOF through a uniform, infinite, straight cylindrical capillary with a wall charge that varies solely in the axial direction. A uniform external electric field and zero imposed pressure gradient was assumed. An exact solution to the Stokes flow problem was derived by means of separation of variables and series expansion. More recently, Herr *et al.* (2000) studied the problem of flow through a cylindrical capillary tube with a wall charge that undergoes a stepwise change in the axial direction. This problem is a special case of that considered by Anderson & Idol. The requirement of mass continuity forces the appearance of a pressure gradient and associated Poiseuille flow. Two capillaries with different surface coatings were joined together to produce a capillary with a stepwise variation in wall charge. The flow profile was measured experimentally using

a caged fluorescence technique, and the result confirmed the theoretical predictions. The problem of electro-osmotic flow between parallel plates was studied by Ajdari (1995, 1996), who considered the simultaneous effect of small periodic deformations of the wall and a periodic distribution of wall charge in the direction of the applied field. It was shown that a net flow and forces could be generated even if the mean charge in the axial direction was zero. Stroock *et al.* (2000) reported observations of electro-osmotic flow in a long channel of rectangular cross-section ($260\,\mu\text{m} \times 130\,\mu\text{m}$) with a patterned surface charge of alternating sign that was fabricated using soft lithographic techniques (Anderson *et al.* 2001). The stripe width was of the same order as the channel width and two orientations were studied, first with stripes parallel to the flow, and secondly, with stripes perpendicular to the flow.

On account of the narrowness of microfluidic channels, axial non-uniformities in wall charge could typically be expected to occur over a characteristic length that is very much larger than a characteristic channel width. This is true, for example, in situations where the variation of wall charge is due to the adsorption of chemicals from the flow stream. Then, the ratio of a characteristic channel width to a characteristic length scale for axial variation is a small parameter, ϵ. An asymptotic solution in the parameter ϵ is presented for the problem of flow through a straight microfluidic channel of arbitrary wall charge and cross-sectional shape at leading order (the lubrication approximation). The solution allows a reduced description of the fluid flow problem in all situations where the lubrication approximation can be justified. In the special case of a channel of circular cross-section with an imposed electric potential but no imposed pressure gradient, the solution of Anderson & Idol quoted above is recovered at leading order. In the case of a channel of circular cross-section with no electric potential but an imposed pressure gradient, we recover the well-known result for pressure-driven flows in capillaries of slowly varying radius (Batchelor 1967). Lubrication theory has been used in the context of electro-osmotic flow by several authors. In particular, Ajdari (1996) considered the lubrication limit of the exact solution to the problem of electro-osmotic flow between two parallel plates in the presence of wall deformations and surface charge that vary in the direction of the electric field. Long, Stone & Ajdari (1999) solved the problem of electro-osmotic flow between parallel plates with arbitrary distribution of the ζ-potential on the two surfaces, and further, considered the lubrication limit of their solution. They also presented the lubrication limit of the exact solution for electro-osmotic flow through a cylindrical capillary with axially varying ζ-potential due to Anderson & Idol (1985). The current analysis differs from the earlier work cited above, in that, the lubrication limit is taken as the starting point of the analysis without any restrictions on the geometry or charge distribution of the channel. Thus, the results presented here have a wider range of validity; in particular, they are applicable to channels of rectangular and trapezoidal cross-sections that are used in practical microfluidic devices. In the special case of parallel plates and cylindrical capillaries, the lubrication limit considered here reduces to the earlier results of Ajdari (1996) and Long *et al.* (1999). The lubrication approximation may not be valid in all problems involving EOF; in particular, it may not be accurate for the case of a stepwise change in wall charge, or a localized source of non-uniformity of dimensions much smaller than the channel diameter. However, in situations where it can be justified, the approximation allows a highly simplified description of the flow. The lubrication approximation has been used effectively in many areas of fluid mechanics; in particular, in the problem of blood flow in microcapillaries (Lighthill 1968; Secomb *et al.* 1986) and more recently, in the analysis of micro-pumps for mechanical pumping of fluids in microfluidic channels (Day & Stone 2000).

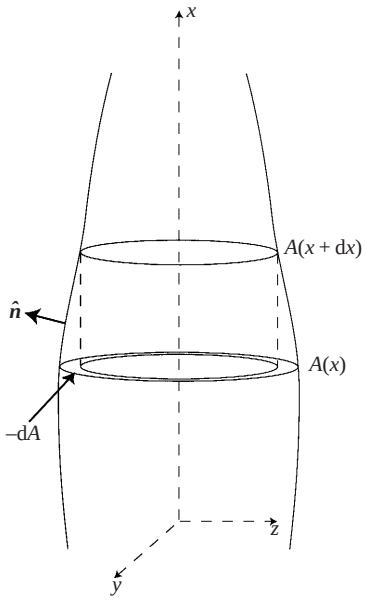

FIGURE 1. The flow geometry for the problem of electro-osmotic flow in a microfluidic channel with variable cross-section and ζ-potential.

In the next section, the basic equations describing the electrohydrodynamic problem in microfluidic channels are written down at the level of the 'Helmholtz–Smoluchowski formulation' for thin Debye layers. In § 3, the lubrication approximation is introduced and the problem is solved by asymptotic analysis in the lubrication limit. In § 4, some of the consequences of the solution are examined in the general case as well as in the particular cases of rectangular and circular cross-sections. For a uniform capillary of circular cross-section, the result of the lubrication analysis is compared to the exact solution for the corresponding Stokes flow problem due to Anderson & Idol. Section 5 contains a summary of the principal results and identifies some possible areas of future investigation.

2. Mathematical formulation

We consider an infinitely long straight channel, or one whose length is very much larger than a characteristic width, which we will denote by a_0. The fluid flow inside the channel will be described by reference to a right-handed orthogonal coordinate system with the x-axis directed along the axis of the channel (figure 1). We make the following assumptions:

(i) The characteristic length scale for the variation of the cross-sectional shape and area in the x-direction is much larger than a_0.

(ii) The characteristic length scale for the variation of the wall charge in the x-direction is much larger than a_0.

(iii) The Debye length (λ_D), characterizing the thickness of the Debye layer, is much smaller than a_0.

The justification for (i) and (ii) was discussed previously. The last assumption is usually a good one, since for typical microfluidic channels, $a_0 \sim 10$–$100\,\mu$m, but $\lambda_D \sim 1$–$10\,$nm.

The fluid velocity, $\boldsymbol{u}$, and pressure p, in the region Ω representing the interior of the channel are governed by the incompressible Navier–Stokes equations and the continuity equation:

$$\rho_0(\partial_t \boldsymbol{u} + \boldsymbol{u} \cdot \nabla \boldsymbol{u}) = -\nabla p + \mu \nabla^2 \boldsymbol{u}, \tag{2.1}$$

$$\nabla \cdot \boldsymbol{u} = 0, \tag{2.2}$$

where, the constants ρ_0 and μ are, respectively, the density and viscosity of the fluid. The electro-osmotic effect arises through the Helmholtz–Smoluchowski slip boundary conditions (Probstein 1994)

$$\left[\boldsymbol{u} + \frac{\kappa \zeta \boldsymbol{E}}{4\pi\mu}\right]_{\partial\Omega} = 0, \tag{2.3}$$

on the part of the boundary $\partial\Omega$ that represents the solid–fluid interface. The constant κ is the dielectric constant of the fluid and $\boldsymbol{E}$ is the electric field outside the Debye layer. This treatment assumes the Debye layer to be infinitely thin, an assumption that may be justified, when $\lambda_D \ll a_0$, so that the velocity at the outer edge of the Debye layer can be used as the boundary condition for the flow in Ω. The parameter ζ, known as the 'ζ-potential', is the electric potential at the inner edge of the Debye layer (Probstein 1994), that is, at the plane corresponding to the true liquid/substrate interface where the 'no slip' boundary conditions for the fluid velocity are imposed. Clearly, it is related to the surface density of fixed charges on the substrate and is determined by the specific surface chemistry of the substrate–electrolyte interface. The assumption of the slow variation of surface charge in the axial direction is equivalent to the assumption that $\zeta = \zeta(x, y, z)$ varies with respect to x on a length scale much larger than a_0. The variation with respect to y and z is, however, arbitrary.

For steady applied voltages, or, if the characteristic time for variation of these voltages is much slower than the characteristic propagation time of electro-magnetic waves over the channel length, the electric field $\boldsymbol{E}$ may be expressed through an electric potential ϕ,

$$\boldsymbol{E} = -\nabla \phi. \tag{2.4}$$

Since the electric double layer at the channel boundary is considered external to the domain Ω, and, the fluid outside the Debye layer is electrically neutral on length scales large in relation to the mean separation of ions, ϕ satisfies

$$\nabla^2 \phi = 0 \tag{2.5}$$

in Ω, with the boundary condition

$$[\hat{\boldsymbol{n}} \cdot \nabla \phi]_{\partial\Omega} = 0, \tag{2.6}$$

where $\hat{\boldsymbol{n}}$ is the unit normal to $\partial\Omega$ directed out of Ω. These boundary conditions must be supplemented with appropriate additional conditions on the lateral boundaries at the inlet and outlet sections S_0 and S_1.

3. Lubrication approximation

Let us denote by L the smallest of the characteristic length scales for the axial variation of the cross-sectional shape, area and ζ-potential. Then, $\epsilon = a_0/L$ is a small parameter of the problem. We would like to obtain the leading-order solution in an asymptotic series in ϵ of the full electrohydrodynamic problem formulated in the previous section.

3.1. *Dimensionless variables*

If ζ_0 and E_0 denote characteristic values for the ζ-potential and electric field, then the fluid velocity in the channel has a characteristic value

$$u_0 = -\frac{\kappa\zeta_0 E_0}{4\pi\mu}. \tag{3.1}$$

The velocity u_0 actually represents exactly the uniform velocity that the fluid will acquire in an infinite uniform channel with no external pressure gradient, but with an imposed constant electric field E_0. Let us introduce the following scaled variables which are expected to be of order unity in the limit $\epsilon \to 0$,

$$X = x/L, \quad Y = y/a_0, \quad Z = z/a_0, \quad T = u_0 t/L, \tag{3.2}$$

$$U = u/u_0, \quad V = (L/a_0)(v/u_0), \quad W = (L/a_0)(w/u_0), \quad P = p/p_0, \tag{3.3}$$

$$\Phi = \phi/(E_0 L), \quad \mathscr{Z} = \zeta/\zeta_0, \tag{3.4}$$

where $p_0 = (\mu u_0 L/a_0^2)$ is a characteristic value for pressure, and the scaling of v and w are chosen so that all of the terms in the continuity equation are of the same order.

In terms of the dimensionless variables, the equations describing the electrohydrodynamic problem presented in the last section take the form

$$\epsilon Re[U_T + UU_X + VU_Y + WU_Z] = -P_X + \epsilon^2 U_{XX} + U_{YY} + U_{ZZ}, \tag{3.5}$$

$$\epsilon Re[V_T + UV_X + VV_Y + WV_Z] = -\frac{1}{\epsilon^2}P_Y + \epsilon^2 V_{XX} + V_{YY} + V_{ZZ}, \tag{3.6}$$

$$\epsilon Re[W_T + UW_X + VW_Y + WW_Z] = -\frac{1}{\epsilon^2}P_Z + \epsilon^2 W_{XX} + W_{YY} + W_{ZZ}, \tag{3.7}$$

$$U_X + V_Y + W_Z = 0, \tag{3.8}$$

$$\epsilon^2\Phi_{XX} + \Phi_{YY} + \Phi_{ZZ} = 0, \tag{3.9}$$

and the boundary conditions on $\partial\Omega$ may be written as

$$[U + \mathscr{Z}\Phi_X]_{\partial\Omega} = 0, \tag{3.10}$$

$$[\epsilon^2 V + \mathscr{Z}\Phi_Y]_{\partial\Omega} = 0, \tag{3.11}$$

$$[\epsilon^2 W + \mathscr{Z}\Phi_Z]_{\partial\Omega} = 0, \tag{3.12}$$

$$[\epsilon^2 \ell\Phi_X + m\Phi_Y + n\Phi_Z]_{\partial\Omega} = 0, \tag{3.13}$$

where $\hat{\boldsymbol{n}} = \epsilon\ell\hat{\boldsymbol{i}} + m\hat{\boldsymbol{j}} + n\hat{\boldsymbol{k}}$ on account of the slow variation in the channel cross-section, and $Re = U_0 a_0 \rho_0/\mu$ is the Reynolds number based on the characteristic channel width. In microfluidic systems the Reynolds number is typically small, $Re \sim 10^{-3}$–10^{-1}. However, the analysis presented here is valid even if $Re \sim 1$, since it depends only on the smallness of the product ϵRe.

3.2. *Asymptotic expansion*

The electrohydrodynamic problem defined above must be solved in the limit of $\epsilon \ll 1$. We expand all dependent variables in asymptotic series in ϵ of the form

$$\Psi = \Psi^{(0)} + \epsilon\Psi^{(1)} + \epsilon^2\Psi^{(2)} + \epsilon^3\Psi^{(3)} + \cdots \tag{3.14}$$

where Ψ stands for any of the variables U, V, W, P or Φ. Equating to zero the coefficient of each term on the left-hand side of the equations, we obtain, at

lowest order

$$-P_X^{(0)} + U_{YY}^{(0)} + U_{ZZ}^{(0)} = 0, \tag{3.15}$$

$$-P_Y^{(0)} = 0, \tag{3.16}$$

$$-P_Z^{(0)} = 0, \tag{3.17}$$

$$U_X^{(0)} + V_Y^{(0)} + W_Z^{(0)} = 0, \tag{3.18}$$

$$\Phi_{YY}^{(0)} + \Phi_{ZZ}^{(0)} = 0, \tag{3.19}$$

and, similarly, from the boundary conditions

$$[U^{(0)} + \mathscr{Z}\Phi_X^{(0)}]_{\partial\Omega} = 0, \tag{3.20}$$

$$[\Phi_Y^{(0)}]_{\partial\Omega} = 0, \tag{3.21}$$

$$[\Phi_Z^{(0)}]_{\partial\Omega} = 0, \tag{3.22}$$

$$[m\Phi_Y^{(0)} + n\Phi_Z^{(0)}]_{\partial\Omega} = 0. \tag{3.23}$$

Equation (3.19), together with boundary condition (3.23), implies that $\Phi^{(0)}$ is a constant with respect to Y and Z. Therefore,

$$\Phi^{(0)} = \Phi^{(0)}(X). \tag{3.24}$$

The conditions (3.21) and (3.22) arising out of the slip boundary conditions on the velocity are therefore identically satisfied. Equations (3.16) and (3.17) imply that

$$P^{(0)} = P^{(0)}(X). \tag{3.25}$$

Let us denote by $D(X)$ the intersection of Ω with the plane perpendicular to the X-axis through the location X, and $\partial D(X)$ the boundary of this domain. Then, the solution of the boundary-value problem (3.15) and (3.20) may be written as

$$U^{(0)} = -\mathscr{P}(X, Y, Z)P_X^{(0)}(X) - \mathscr{E}(X, Y, Z)\Phi_X^{(0)}(X), \tag{3.26}$$

where $\mathscr{P}$ and $\mathscr{E}$ are defined through the following boundary-value problems on the two-dimensional domain $D(X)$ and have only a parametric dependence on X:

$$\mathscr{P}_{YY} + \mathscr{P}_{ZZ} = -1, \tag{3.27}$$

$$\mathscr{P}|_{\partial D(X)} = 0, \tag{3.28}$$

and

$$\mathscr{E}_{YY} + \mathscr{E}_{ZZ} = 0, \tag{3.29}$$

$$\mathscr{E}|_{\partial D(X)} = \mathscr{Z}. \tag{3.30}$$

If we introduce the Green function, $G(X; Y, Z, Y_*, Z_*)$ for the Laplace operator in $D(X)$ corresponding to zero boundary conditions on $\partial D(X)$:

$$\frac{\partial^2 G}{\partial Y_*^2} + \frac{\partial^2 G}{\partial Z_*^2} = -4\pi\delta(Y_* - Y)\delta(Z_* - Z), \tag{3.31}$$

$$G(X; Y, Z, Y_*, Z_*)|_{(Y_*, Z_*)\in\partial D(X)} = 0, \tag{3.32}$$

both $\mathscr{P}$ and $\mathscr{E}$ may be expressed in terms of G as follows:

$$\mathscr{P} = \frac{1}{4\pi}\int_{D(X)} G(X; Y, Z, Y_*, Z_*)\,\mathrm{d}Y_*\,\mathrm{d}Z_*, \tag{3.33}$$

$$\mathscr{E} = -\frac{1}{4\pi}\oint_{\partial D(X)} \mathscr{Z}(X, Y_*, Z_*)\left(m\frac{\partial G}{\partial Y_*} + n\frac{\partial G}{\partial Z_*}\right)\mathrm{d}S_*. \tag{3.34}$$

Although (3.26) gives the solution to our electrohydrodynamic problem at leading order, it is incomplete as it still involves two unknown functions of X, $P^{(0)}(X)$ and $\Phi^{(0)}(X)$. To determine these we must examine the solvability conditions of the higher-order equations in the asymptotic development. This is considered next.

3.3. *Solvability conditions*

To obtain the solvability condition for $\Phi^{(0)}$ we must consider the order ϵ^2 term in the asymptotic expansion for (3.9) and (3.13):

$$\Phi^{(2)}_{YY} + \Phi^{(2)}_{ZZ} = -\Phi^{(0)}_{XX}(X), \tag{3.35}$$

$$\left[m\Phi^{(2)}_{Y} + n\Phi^{(2)}_{Z} + \ell\,\Phi^{(0)}_{X}(X)\right]_{\partial D(X)} = 0. \tag{3.36}$$

Clearly, the right-hand side of (3.35) and the boundary value of the normal derivative $m\Phi^{(2)}_{Y} + n\Phi^{(2)}_{Z}$ cannot be arbitrarily specified, since, $\Phi^{(2)}$ must obey the condition

$$\int_{D(X)} (\Phi^{(2)}_{YY} + \Phi^{(2)}_{ZZ})\,\mathrm{d}Y\,\mathrm{d}Z = \oint_{\partial D(X)} (m\Phi^{(2)}_{Y} + n\Phi^{(2)}_{Z})\,\mathrm{d}s, \tag{3.37}$$

obtained by applying the divergence theorem to the vector $\Phi^{(2)}_{Y}\hat{\boldsymbol{j}} + \Phi^{(2)}_{Z}\hat{\boldsymbol{k}}$ in the domain $D(X)$. Using (3.35) and (3.36) in (3.37) we obtain a solvability condition for $\Phi^{(2)}$,

$$\Phi^{(0)}_{XX}(X) \int_{D(X)} \mathrm{d}Y\,\mathrm{d}Z = \Phi^{(0)}_{X}(X) \oint_{\partial D(X)} \ell\,\mathrm{d}s, \tag{3.38}$$

which determines $\Phi^{(0)}$. The integral on the left-hand side is the dimensionless area of the cross-section of the channel at axial location X;

$$\mathscr{A}(X) = \int_{D(X)} \mathrm{d}Y\,\mathrm{d}Z, \tag{3.39}$$

the integral on the right-hand side also has a simple geometrical meaning. From figure 1, the change in cross-sectional area between the axial locations X and $X + \mathrm{d}X$ is equal to the projection on the (Y, Z)-plane of the section of the channel wall that lies between these cross-sections. Thus,

$$-\mathrm{d}\mathscr{A} = \oint_{\partial D(X)} \hat{\boldsymbol{n}} \cdot \hat{\boldsymbol{i}}\,(\mathrm{d}X)\,\mathrm{d}s = (\mathrm{d}X) \oint_{\partial D(X)} \ell\,\mathrm{d}s, \tag{3.40}$$

or

$$-\frac{\mathrm{d}\mathscr{A}}{\mathrm{d}X} = \oint_{\partial D(X)} \ell\,\mathrm{d}s. \tag{3.41}$$

Using (3.39) and (3.41) in (3.38) we obtain

$$\Phi^{(0)}_{XX}(X)\mathscr{A} + \Phi^{(0)}_{X}(X)\mathscr{A}_X = 0, \tag{3.42}$$

or

$$\frac{\mathrm{d}}{\mathrm{d}X}\left(\mathscr{A}\Phi^{(0)}_{X}\right) = 0, \tag{3.43}$$

or

$$-\Phi^{(0)}_{X}(X)\mathscr{A}(X) = \mathscr{F}, \tag{3.44}$$

where $\mathscr{F}$ is a constant. Equation (3.44) which determines $\Phi^{(0)}$ corresponds physically to 'Gauss's law' of electrostatics, namely, the net electric flux through the boundaries of a charge-free domain must be zero. Equation (3.44) may be integrated to determine

Φ_0 in terms of two arbirary constants which may be determined, for example, if the electric potentials at the inlet and outlet sections are specified.

To determine the unknown pressure distribution $P^{(0)}(X)$, we consider equation (3.18)

$$V_Y^{(0)} + W_Z^{(0)} = -U_X^{(0)}, \tag{3.45}$$

and the order ϵ^2 terms in the boundary conditions (3.11) and (3.12),

$$\left[V^{(0)} + \mathscr{Z}\Phi_Y^{(2)}\right]_{\partial\Omega} = 0, \tag{3.46}$$

$$\left[W^{(0)} + \mathscr{Z}\Phi_Z^{(2)}\right]_{\partial\Omega} = 0, \tag{3.47}$$

Equations (3.46), (3.47) and (3.36) imply

$$[mV^{(0)} + nW^{(0)} + \mathscr{Z}(m\Phi_Y^{(2)} + n\Phi_Z^{(2)})]_{\partial D(X)} = [mV^{(0)} + nW^{(0)} - \mathscr{Z}\ell\Phi_X^{(0)}]_{\partial D(X)} = 0. \tag{3.48}$$

Equation (3.45) and the boundary condition (3.48) are compatible only if the divergence theorem in the two-dimensional domain $D(X)$:

$$\int_{D(X)} (V_Y^{(0)} + W_Z^{(0)})\,\mathrm{d}Y\,\mathrm{d}Z = \oint_{\partial D(X)} (mV^{(0)} + nW^{(0)})\,\mathrm{d}s, \tag{3.49}$$

is satisfied. On using (3.45) and (3.48) in (3.49) we obtain

$$\int_{D(X)} U_X^{(0)}\,\mathrm{d}Y\,\mathrm{d}Z = -\Phi_X^{(0)} \oint_{\partial D(X)} \ell\mathscr{Z}\,\mathrm{d}s. \tag{3.50}$$

This relation may be rewritten in a form that would make its physical content more intuitive. Since the domain $D(X)$ varies in the X-direction we have

$$\frac{\mathrm{d}}{\mathrm{d}X}\int_{D(X)} U^{(0)}\,\mathrm{d}Y\,\mathrm{d}Z = \int_{D(X)} \frac{\partial U^{(0)}}{\partial X}\,\mathrm{d}Y\,\mathrm{d}Z - \oint_{\partial D(X)} \ell U^{(0)}\,\mathrm{d}s, \tag{3.51}$$

$-\ell\,\mathrm{d}X\,\mathrm{d}s$ being the differential area element that makes up the annular region between $D(X)$ and $D(X + \mathrm{d}X)$. Now using the boundary condition (3.20), (3.50) may be rewritten as

$$\int_{D(X)} U_X^{(0)}\,\mathrm{d}Y\,\mathrm{d}Z - \oint_{\partial D(X)} \ell U^{(0)}\,\mathrm{d}s = 0, \tag{3.52}$$

so that, on using (3.51) for differentiating under the integral sign, we have

$$\frac{\mathrm{d}}{\mathrm{d}X}\int_{D(X)} U^{(0)}\,\mathrm{d}Y\,\mathrm{d}Z = 0. \tag{3.53}$$

If we substitute the expression (3.26) for $U^{(0)}$ in the above equation and use (3.44), we obtain

$$\frac{\mathrm{d}}{\mathrm{d}X}\left[-P_X^{(0)}(X)\int_{D(X)} \mathscr{P}\,\mathrm{d}Y\,\mathrm{d}Z + \frac{\mathscr{F}}{\mathscr{A}(X)}\int_{D(X)} \mathscr{E}\,\mathrm{d}Y\,\mathrm{d}Z\right] = 0, \tag{3.54}$$

so that,

$$-P_X^{(0)}(X)\int_{D(X)} \mathscr{P}\,\mathrm{d}Y\,\mathrm{d}Z + \frac{\mathscr{F}}{\mathscr{A}(X)}\int_{D(X)} \mathscr{E}\,\mathrm{d}Y\,\mathrm{d}Z = \mathscr{Q}, \tag{3.55}$$

where $\mathscr{Q}$ is a constant. Equation (3.55) or its equivalent (3.53) is simply the statement of conservation of volume flux and $\mathscr{Q}$ represents the lowest-order approximation to

the dimensionless volume flux. Equation (3.55) determines the pressure distribution given the inlet pressure and the volume flux. Alternatively, given both the inlet and outlet pressures, this equation determines the volume flux of fluid through the channel.

3.4. *Summary of solution*

The solution in the lubrication limit obtained above is summarized below and expressed in physical units for convenience in applications. Since the cross-channel velocity components are of order ϵ compared to the axial component, we have, $\boldsymbol{u} \sim \hat{\boldsymbol{i}} u(x, y, z) + O(\epsilon)$. On expressing (3.26), (3.44) and (3.55) in physical units, we have the following solution for the velocity, $\boldsymbol{u}$, pressure, p, and the electric field, $\boldsymbol{E} \sim \hat{\boldsymbol{i}} E(x) + O(\epsilon)$,

$$u = -\frac{u_p}{\mu}\frac{\mathrm{d}p}{\mathrm{d}x} + \frac{\kappa F}{4\pi\mu}\frac{\psi}{A(x)}, \tag{3.56}$$

$$Q = -\frac{\bar{u}_p}{\mu}A(x)\frac{\mathrm{d}p}{\mathrm{d}x} + \frac{\kappa F\bar{\psi}}{4\pi\mu}, \tag{3.57}$$

$$E(x) = F/A(x). \tag{3.58}$$

Here, F is a constant representing the electric flux through any cross-section, $A(x)$ is the cross-sectional area and the overbar indicates the average over the cross-section, $\bar{f} = A^{-1}\int f \,\mathrm{d}y\,\mathrm{d}z$. The constant Q represents the volume flux of fluid through any cross-section, the dielectric constant and the dynamic viscosity are, respectively, κ and μ. The functions u_p and ψ are defined by the scaled versions of (3.27), (3.28), (3.29) and (3.30):

$$\frac{\partial u_p}{\partial y^2} + \frac{\partial u_p}{\partial z^2} = -1, \tag{3.59}$$

$$u_p|_{\partial D(x)} = 0, \tag{3.60}$$

and

$$\frac{\partial \psi}{\partial y^2} + \frac{\partial \psi}{\partial z^2} = 0, \tag{3.61}$$

$$\psi|_{\partial D(x)} = -\zeta. \tag{3.62}$$

Both of these functions u_p and ψ may be evaluated by quadrature from a knowledge of the Green function, G, of the Laplace operator with zero boundary condition corresponding to the domain $D(x)$;

$$u_p = \frac{1}{4\pi}\int_{D(x)} G(x; y, z, y_*, z_*)\,\mathrm{d}y_*\,\mathrm{d}z_*, \tag{3.63}$$

$$\psi = \frac{1}{4\pi}\oint_{\partial D(x)} \zeta(x, y_*, z_*)\left(m\frac{\partial G}{\partial y_*} + n\frac{\partial G}{\partial z_*}\right)\mathrm{d}s_*. \tag{3.64}$$

The physical content of the solution (3.56)–(3.58) is clear. If the properties of the channel vary slowly in the axial direction, then, according to (3.56), the flow velocity, to a first approximation, is purely axial, and it may be expressed as a linear superposition of a purely pressure-driven flow and a purely electro-osmotic flow. Further, in calculating the local electro-osmotic flow component we must use an effective ζ-potential ψ which is a certain weighted average, (3.64), of the actual ζ-potential around the contour of the cross-section. The pressure-driven component and the electro-osmotic component are proportional to the local pressure gradient and

the local electric field strength, respectively. The local pressure gradient is calculated by using the condition (3.57) for volume conservation of fluid, and the local electric field is calculated by using the condition (3.58) for electric flux conservation. The solution is completely specified by two independent physical constants, the volume flux of fluid, Q, and, the flux of electric field, F. These constants may be expressed, if desired, in terms of the total pressure drop and the total voltage drop, respectively, between the inlet and outlet sections.

4. Applications

In this section, some applications of the lubrication solution presented above in general as well as special geometries are indicated.

Let us suppose, that the inlet and exit pressures, p_a and p_b, are given, together with the inlet and outlet voltages, V_a and V_b. If we integrate (3.58) along the channel, we obtain

$$V_a - V_b = \int_{x_a}^{x_b} E(x)\,\mathrm{d}x = FL\langle A^{-1}\rangle, \tag{4.1}$$

where $x = x_a$ and $x = x_b$ correspond to the inlet and outlet sections and $L = x_b - x_a$ is the channel length. We have used the notation $\langle\ \ \rangle$ to indicate average in the axial direction, $\langle\cdots\rangle = L^{-1}\int_{x_a}^{x_b}(\cdots)\,\mathrm{d}x$. If we solve (3.57) for $\mathrm{d}p/\mathrm{d}x$ and integrate along the channel, we obtain

$$p_a - p_b = -\int_{x_a}^{x_b} \frac{\mathrm{d}p}{\mathrm{d}x}\,\mathrm{d}x = \mu QL\langle \bar{u}_p^{-1}A^{-1}\rangle - \frac{\kappa FL}{4\pi}\langle A^{-1}\bar{u}_p^{-1}\bar{\psi}\rangle. \tag{4.2}$$

If we use (4.1) in (4.2) to eliminate F and rewrite the resulting equation with Q on the left-hand side, we obtain an expression for the volume flow rate in the channel in terms of the applied pressure and voltage difference:

$$Q = \frac{p_a - p_b}{\mu L}\frac{1}{\langle \bar{u}_p^{-1}A^{-1}\rangle} + \frac{\kappa}{4\pi\mu}\frac{\langle \bar{u}_p^{-1}A^{-1}\bar{\psi}\rangle}{\langle A^{-1}\rangle\langle \bar{u}_p^{-1}A^{-1}\rangle}\frac{V_a - V_b}{L}. \tag{4.3}$$

If we introduce the notation

$$a_* = \left[\frac{8}{\pi\langle \bar{u}_p^{-1}A^{-1}\rangle}\right]^{1/4}, \tag{4.4}$$

$$\zeta_* = -\frac{1}{\sqrt{8\pi}}\frac{\langle \bar{\psi}\bar{u}_p^{-1}A^{-1}\rangle}{\langle A^{-1}\rangle\langle \bar{u}_p^{-1}A^{-1}\rangle^{1/2}}, \tag{4.5}$$

then, (4.3) may be written as

$$Q = \frac{p_a - p_b}{8\mu L}\pi a_*^4 - \frac{\kappa\zeta_*}{4\pi\mu}\pi a_*^2\frac{V_a - V_b}{L}. \tag{4.6}$$

The last equation shows that, within the limits of validity of the lubrication approximation, the volume flux through any straight microfluidic channel is equal to that of the flux through a cylindrical capillary of uniform radius a_* and uniform ζ-potential ζ_* which is subject to an identical pressure and voltage drop. The 'effective' values of the radius, a_*, and, ζ-potential, ζ_*, are given by (4.4) and (4.5), and are seen to depend purely on the geometry of the channel and the charge distribution on its walls. The concept of the effective radius and effective ζ-potential could be useful in the analysis of microfluidic circuit components, and could be considered analogous to the concept

of 'impedance' in electric circuit theory. Specific examples of computation of a_* and ζ_* are provided later.

Numerical solution of the electrohydrodynamical equations is often necessary in order to optimize the design of microfluidic devices (Patankar & Hu 1998). For flow in straight channels where the lubrication approximation is justified, (3.56)–(3.58) provide a greatly simplified approach to computing the flow than solving the full three-dimensional partial differential equations describing the problem. In the lubrication formalism, we need only solve the sequence of two-dimensional problems defined by (3.59)–(3.62). Further, if the cross-sectional shapes and boundary distribution of ζ-potential at different axial locations can be made congruent through a similarity transformation, the two-dimensional boundary-value problems (3.59)–(3.62) need only be solved once rather than for each x location. Furthermore, for certain cross-sectional shapes the Green function G or equivalently the solutions ψ and u_p may be available in analytical form. In such cases, the flow field may be obtained simply through algebraic evaluations without numerically integrating partial differential equations. Some analytically solvable examples will be considered below.

4.1. *Circular capillaries*

Let us consider a channel with circular cross-section, the radius being $a(x)$. The length scale, Δx over which $a(x)$ varies significantly is assumed to be very much larger than the largest value of $a(x)$. The boundary-value problems for u_p for all cross-sections may be made congruent through the similarity transformation

$$u_p = a^2(x) U_p(\rho), \tag{4.7}$$

$$\rho = r/a(x), \tag{4.8}$$

and the resulting equation for $U_p(\rho)$ may be integrated to give

$$U_p(\rho) = \tfrac{1}{4}\left(1 - \rho^2\right). \tag{4.9}$$

The equation for ψ may be solved in cylindrical coordinates (r, θ, x) as

$$\psi = -\bar{\zeta} - \sum_{m=1}^{\infty} [\tilde{\zeta}_m \exp(\mathrm{i}m\theta) + \tilde{\zeta}_m^* \exp(-\mathrm{i}m\theta)]\rho^m, \tag{4.10}$$

where $\tilde{\zeta}_m$ is the complex Fourier transform:

$$\tilde{\zeta}_m = \frac{1}{2\pi} \int_0^{2\pi} \zeta(x, \theta) \exp(-\mathrm{i}m\theta)\, \mathrm{d}\theta, \tag{4.11}$$

and $\bar{\zeta} = \tilde{\zeta}_0$ is the ζ-potential averaged over the perimeter. (An overbar will indicate cross-sectional average except where the variable is defined only on the boundary of the cross-section in which case it would indicate the average over the perimeter.) From (4.10) we have

$$\bar{\psi} = -\bar{\zeta}(x), \tag{4.12}$$

so that (4.4) and (4.5) may be evaluated to give the following expressions for the effective radius and ζ-potential

$$a_* = \frac{1}{\langle a^{-4} \rangle^{1/4}}, \tag{4.13}$$

$$\zeta_* = \frac{\langle \bar{\zeta} a^{-4} \rangle}{\langle a^{-2} \rangle \langle a^{-4} \rangle^{1/2}}. \tag{4.14}$$

Note that equation (4.14) implies that, in the lubrication limit, the volume flux through the channel is independent of the azimuthal distribution of the ζ-potential.

In the absence of an applied voltage, (4.6) and (4.13) give the well-known (Batchelor 1967) result for pressure-driven flows in slowly varying channels

$$p_a - p_b = \frac{8\mu Q}{\pi} \int_{x_a}^{x_b} \frac{\mathrm{d}x}{a^4(x)}. \tag{4.15}$$

When there is no external pressure difference, $p_a = p_b$, (4.6), (4.13) and (4.14) imply

$$Q = -\frac{\kappa}{4\mu} \frac{\langle \bar{\zeta} a^{-4} \rangle}{\langle a^{-4} \rangle \langle a^{-2} \rangle} \frac{V_a - V_b}{L}. \tag{4.16}$$

The problem of electro-osmotic flow through a uniform ($a(x) = a_0$) capillary, with no externally imposed pressure gradient, and a ζ-potential depending only on the axial direction, $\zeta = \zeta(x)$, admits an exact solution (Anderson & Idol 1985) in the Stokes flow limit ($Re = u_0 a_0 \rho_0 / \mu \to 0$). This solution, which is discussed further later in this section, gives the following result for the volume flux

$$Q = -\frac{\kappa \langle \zeta \rangle}{4\pi\mu} \frac{V_a - V_b}{L} \pi a_0^2, \tag{4.17}$$

which is seen to be identical to (4.16) when ζ is independent of θ and $a(x)$ is independent of x. Note, however, (4.17) follows from an exact solution to the Stokes equation and is valid even when $\zeta(x)$ varies rapidly so that the lubrication approximation is not applicable.

A few special cases of channels with circular cross-section are now considered in order to demonstrate the usefulness of these results. In all of the special cases that follow, the ζ-potential is assumed to vary only in the axial direction.

4.1.1. *Capillaries of uniform radius*

When $a(x) = a_0$ and $\zeta = \zeta(x)$, (4.10) reduces to $\psi = -\zeta(x)$, and, on using (4.8), the lubrication equations presented in § 3.4 reduce to

$$u = -\frac{a_0^2 - r^2}{4\mu} \frac{\mathrm{d}p}{\mathrm{d}x} - \frac{\kappa \zeta(x) E}{4\pi\mu}, \tag{4.18}$$

$$Q = -\frac{a_0^2}{8\mu} \pi a_0^2 \frac{\mathrm{d}p}{\mathrm{d}x} - \frac{\kappa \zeta(x) E}{4\pi\mu} \pi a_0^2, \tag{4.19}$$

where $E = (V_a - V_b)/L$ is the uniform electric field in the capillary. Equation (4.19) may be solved for $\mathrm{d}p/\mathrm{d}x$,

$$\frac{\mathrm{d}p}{\mathrm{d}x} = -\frac{8\mu Q}{\pi a_0^4} - \frac{2\kappa \zeta(x) E}{\pi a_0^2}. \tag{4.20}$$

If no external pressure head is imposed, this equation may be integrated with boundary condition $p_a = p_b$, which gives (4.17) for the volume flux. Therefore, the pressure gradient and axial velocity may be written as

$$\frac{\mathrm{d}p}{\mathrm{d}x} = \frac{8\mu u_0}{a_0^2} \left(\frac{\zeta}{\langle \zeta \rangle} - 1 \right), \tag{4.21}$$

$$\frac{u}{u_0} = \frac{\zeta(x)}{\langle \zeta \rangle} + 2 \left(1 - \frac{\zeta(x)}{\langle \zeta \rangle} \right) \left(1 - \frac{r^2}{a_0^2} \right). \tag{4.22}$$

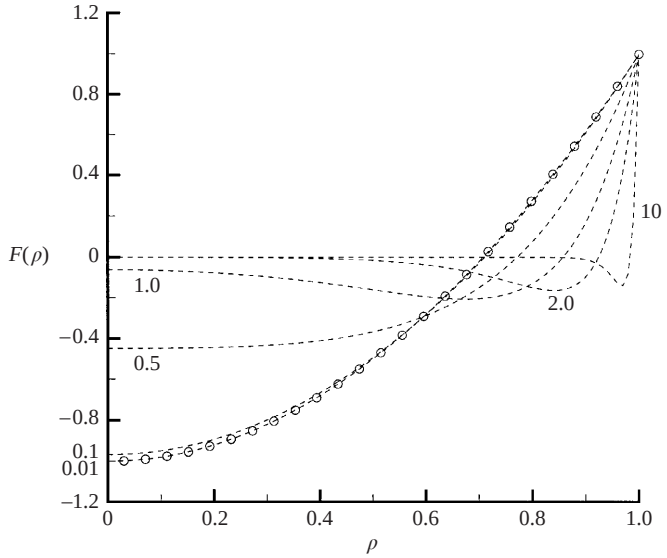

FIGURE 2. Comparison of the asymptotic solution in the lubrication limit (symbols) with the exact solution (dashed lines) due to Anderson & Idol. The ratio of channel radius to wavelength, a_0/λ, is indicated near the respective curves, the asymptotic solution corresponds to $a_0/\lambda \to 0$.

As a special case of an axially varying ζ-potential, let us consider

$$\zeta(x) = \zeta_0 + \Delta\zeta \sin\left(2\pi\frac{x}{\lambda}\right), \tag{4.23}$$

where λ and $\Delta\zeta$ are the wavelength and amplitude of the fluctuations. We then obtain from the lubrication solution (4.22)

$$\frac{u}{u_0} = 1 + \frac{\Delta\zeta}{\zeta_0} F_0(\rho)\sin(\alpha X), \tag{4.24}$$

where

$$F_0(\rho) = 2\rho^2 - 1. \tag{4.25}$$

Here, $\rho = r/a_0$ and $X = x/a_0$ are dimensionless radial and axial coordinates and $\alpha = 2\pi(a_0/\lambda)$ is the appropriate parameter characterizing the lubrication limit ($\alpha \ll 1$). The exact solution corresponding to the distribution (4.23) in the Stokes flow limit may be written down as a special case of the series solution presented by Anderson & Idol:

$$\frac{u}{u_0} = 1 + \frac{\Delta\zeta}{\zeta_0} F(\rho)\sin(\alpha X), \tag{4.26}$$

where

$$F(\rho) = \frac{\alpha^{-1} I_0(\alpha\rho)[1 - \alpha I_0(\alpha)/2I_1(\alpha)] + (\rho/2) I_1(\alpha\rho)}{\alpha^{-1} I_0(\alpha) + \frac{1}{2} I_1(\alpha) - I_0^2(\alpha)/2I_1(\alpha)}. \tag{4.27}$$

Here, I_0 and I_1 are the modified Bessel functions of order zero and one, respectively. In the limit of small α, we may replace I_0 and I_1 by their asymptotic forms for small argument (Abramowitz & Stegun 1970), so that we may readily verify

$$\lim_{\alpha\to 0} F(\rho) = 2\rho^2 - 1 = F_0(\rho), \tag{4.28}$$

which is consistent with (4.25) derived using lubrication theory.

Figure 2 compares $F(\rho)$ and $F_0(\rho)$ for several values of the ratio a_0/λ. It is seen, that, for $a_0/\lambda = 0.1$ or less, the prediction of the lubrication analysis is in excellent accord with the exact solution. For $a_0/\lambda \sim 1$, the exact solution deviates significantly from the lubrication solution. In the opposite limit of $a_0/\lambda \gg 1$, the exact solution is seen to be of the nature of a boundary layer, where the bulk flow in the tube is almost identical to a plug flow with uniform ζ-potential $\zeta = \zeta_0$, and the effect of the fluctuations in the ζ-potential is felt only in a thin shear layer very close to the wall.

4.1.2. *Capillaries with corrugated walls*

Equations (4.13) and (4.14) for the effective radius and cross-section can be used to illustrate an effect that appears to have been first noted by Ajdari (1995, 1996). Since (4.14) involves an axial average of $\bar{\zeta}$ weighted by certain powers of $a(x)$, it is quite possible to have a net flow ($\zeta_* \neq 0$), even though $\langle\bar{\zeta}\rangle = 0$. The result is generally true, even for capillaries of non-circular cross-section, since, on replacing $\bar{\psi}$ in (4.5) by (3.64), it is seen that $\langle\bar{\zeta}\rangle = 0$ in general does not guarantee $\zeta_* = 0$. Physically, the effect comes about as a consequence of the conservation of electric flux. The electric field is amplified in narrow sections of the tube inversely as the area, so that more momentum is transferred to the free charges in the Debye layer in narrow sections of the tube than in the wider sections even though the charge per unit length in the wide and narrow sections may be the same. The effect is of relevance to some models of the propulsion mechanism in certain cells (Lammert, Prost & Bruinsma 1996) and in the bacterial flagellar motor (Berry 1993).

As a specific example, let us consider a corrugated channel

$$a(x) = a_0 + \Delta a \sin\left(\frac{2\pi}{\lambda}x\right), \tag{4.29}$$

and a distribution of ζ-potential such that

$$\bar{\zeta} = \zeta_0 \sin\left(\frac{2\pi}{\lambda}x + \phi\right), \tag{4.30}$$

(of course, if the charge distribution is axially symmetric, $\bar{\zeta} = \zeta$). The effective ζ-potential, ζ_*, may be obtained by substitution of these relations in (4.14), the integrals involved in the averaging operator is best evaluated numerically. If $\Delta a \ll a_0$, (4.14) may be evaluated by linearizing in $\Delta a/a_0$:

$$\zeta_* \approx -2\zeta_0 \frac{\Delta a}{a_0}\cos\phi, \tag{4.31}$$

which is a good approximation when $\Delta a \ll a_0$. Therefore, in the absence of an imposed pressure head ($p_a = p_b$), the dimensionless fluid flux is

$$\frac{Q}{u_0 \pi a_0^2} = -2\frac{\Delta a}{a_0}\cos\phi, \tag{4.32}$$

where $u_0 = -(\kappa\zeta_0 E)/(4\pi\mu)$, $E = (V_a - V_b)/L$. Figure 3 shows $Q/(u_0\pi a_0^2)$ divided by $\Delta a/a_0$ as a function of the phase difference ϕ between the waves of wall deformation and electric charge, evaluated using the expression (4.14) as well as the approximate form (4.32) valid for small deformation. It is seen that the volume flux has the largest positive value when the two waves are exactly out of phase ($\phi = \pi$) and the smallest negative value when they are in phase ($\phi = 0, 2\pi$). The linearized theory, (4.32), is a good approximation for $\Delta a/a_0 \sim 0.1$; however, for $\Delta a/a_0 \sim 1$, it overpredicts the flow

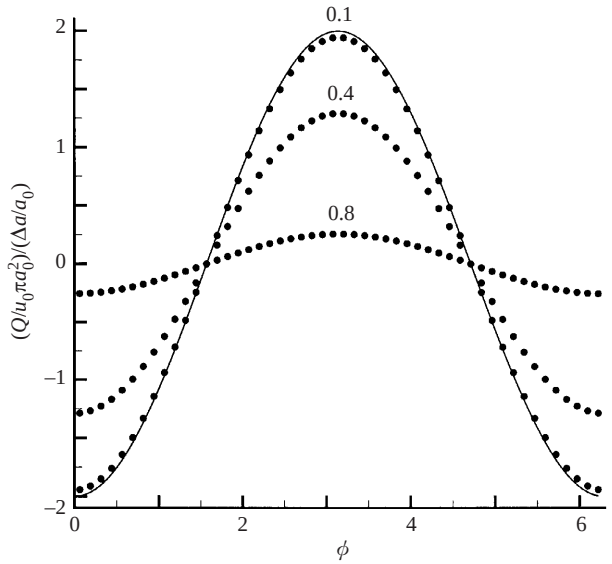

FIGURE 3. The normalized volume flux per unit amplitude as a function of the phase difference ϕ between the wall deformation and the ζ-potential for various values of the amplitude $\Delta a/a_0$ in the case of a cylindrical capillary with wavy walls. Symbols indicate the result of using equation (4.14) and the solid line corresponds to the small-amplitude approximation to it, equation (4.32).

rate. The result of using (4.14), denoted by the symbols, should be accurate for large or small values of $\Delta a/a_0$ since its accuracy is only determined by the validity of the lubrication approximation, $\lambda \gg a_0$.

Ajdari (1995, 1996) demonstrated this effect by considering the problem of electro-osmotic flow between a plane and a slightly wavy wall with a sinusoidal distribution of wall ζ-potential along one of the walls. An explanation of the effect is presented here within the framework of lubrication theory for channels of arbitrary cross-sectional shapes and wall charge distributions. An explicit calculation illustrating this was shown for capillaries of circular cross-section, and, later, for flow between parallel walls.

4.2. *Channels of rectangular cross-section*

Cylindrical capillaries are commonly used for capillary electrophoresis. However, microfluidic circuits are usually produced by etching on a substrate, so that the channel cross-sections are generally trapezoidal or rectangular in shape. We therefore consider a channel of rectagular cross-section, the length of the edges being $2b$ and $2c$. In general, b and c could vary in x, and, further, the orientation of the rectangle could change with x. It is only required that the length scale for any such variation be much larger than the maximum value of c or b. The distribution of ζ-potential can be completely arbitrary, except that, if it varies in the x-direction, such variation must be 'slow' in the above sense.

In the lubrication approximation, the problem reduces to determining the functions u_p and ψ at every axial location x. Without loss of generality, we may choose the y- and z-axes along the edges of the rectangle, so that $b \geqslant y \geqslant -b$ and $c \geqslant z \geqslant -c$ define the channel cross-section. Fortunately, the functions u_p and ψ can be determined analytically for arbitrary ζ-potential distributions along the edges of the rectangle.

Equations (3.59) and (3.60) admit an analytical solution (Whitham 1963) for

rectangular cross-section

$$u_p(y,z) = \tfrac{1}{2}b^2 - \tfrac{1}{2}y^2 - 2b^2\left(\frac{2}{\pi}\right)^3 \sum_{n=0}^{\infty} \frac{(-1)^n}{(2n+1)^3} \frac{\cosh[(2n+1)(\pi z/2b)]}{\cosh[(2n+1)(\pi c/2b)]} \cos[(2n+1)(\pi y/2b)]. \tag{4.33}$$

The solution can be integrated over the cross-section to find the flux,

$$4bc\,\bar{u}_p = \tfrac{4}{3}cb^3 - 8b^4\left(\frac{2}{\pi}\right)^3 \sum_{n=0}^{\infty} \frac{1}{(2n+1)^5} \tanh\left[(2n+1)\frac{\pi c}{2b}\right]. \tag{4.34}$$

In the special cases $b \approx c$ and $b \ll c$, we have the useful asymptotic forms

$$4bc\bar{u}_p \sim \begin{cases} 0.5623\,b^4 & \text{if } c \approx b \\ cb^3\left(\frac{4}{3} - 0.840b/c\right) & \text{if } c \gg b. \end{cases} \tag{4.35}$$

Incidentally, the asymptotic form for $c \gg b$ given above, is accurate to within 10% as long as $b < 0.7c$ (Anderson *et al.* 2001).

The problem for ψ involves solving the harmonic equation in a rectangular domain with Dirichlet boundary condition $\psi = -\zeta$ where

$$\zeta \sim \begin{cases} \zeta_h^-(y) & \text{if } z = -c, \\ \zeta_h^+(y) & \text{if } z = +c, \\ \zeta_v^-(z) & \text{if } y = -b, \\ \zeta_v^+(z) & \text{if } y = +b, \end{cases} \tag{4.36}$$

where ζ_h^-, ζ_h^+, ζ_v^- and ζ_v^+ are arbitrary functions of y or z. They could also depend on x, though the x-dependence is not shown explicitly for brevity. Owing to the linearity of the Dirichlet problem, the solution may be written as

$$\psi = \psi_h^- + \psi_h^+ + \psi_v^- + \psi_v^+, \tag{4.37}$$

where ψ_h^- is the solution of the Dirichlet problem with $\zeta = \zeta_h^-$ on the $z = -c$ boundary and $\zeta = 0$ on the remaining three sides, and ψ_h^+, ψ_v^- and ψ_v^+ are defined by analogy, and correspond to the sides $z = +c$, $y = -b$ and $y = +b$, respectively. The solution to any one of the four problems can be obtained readily using the method of separation of variables, and the remaining solutions may be written down from symmetry. Thus,

$$\psi_h^-(y,z) = \sum_{n=1}^{\infty} \tilde{\zeta}_h^-(n) \frac{\sinh\left[\frac{n\pi}{2b}(z-c)\right]}{\sinh\left(\frac{n\pi c}{b}\right)} \sin\left[\frac{n\pi}{2b}(y+b)\right], \tag{4.38}$$

$$\psi_h^+(y,z) = -\sum_{n=1}^{\infty} \tilde{\zeta}_h^+(n) \frac{\sinh\left[\frac{n\pi}{2b}(z+c)\right]}{\sinh\left(\frac{n\pi c}{b}\right)} \sin\left[\frac{n\pi}{2b}(y+b)\right], \tag{4.39}$$

$$\psi_v^-(y,z) = \sum_{n=1}^{\infty} \tilde{\zeta}_v^-(n) \frac{\sinh\left[\frac{n\pi}{2c}(y-b)\right]}{\sinh\left(\frac{n\pi b}{c}\right)} \sin\left[\frac{n\pi}{2c}(z+c)\right], \tag{4.40}$$

$$\psi_v^+(y,z) = -\sum_{n=1}^{\infty} \tilde{\zeta}_v^+(n) \frac{\sinh\left[\frac{n\pi}{2c}(y+b)\right]}{\sinh\left(\frac{n\pi b}{c}\right)} \sin\left[\frac{n\pi}{2c}(z+c)\right], \tag{4.41}$$

where

$$\tilde{\zeta}_v^-(n) = \frac{1}{c}\int_{-c}^{+c} \zeta_v^-(z)\sin\left[\frac{n\pi}{2c}(z+c)\right]\,\mathrm{d}z, \tag{4.42}$$

$$\tilde{\zeta}_v^+(n) = \frac{1}{c}\int_{-c}^{+c} \zeta_v^+(z)\sin\left[\frac{n\pi}{2c}(z+c)\right]\,\mathrm{d}z, \tag{4.43}$$

$$\tilde{\zeta}_h^-(n) = \frac{1}{b}\int_{-b}^{+b} \zeta_h^-(y)\sin\left[\frac{n\pi}{2b}(y+b)\right]\,\mathrm{d}y, \tag{4.44}$$

$$\tilde{\zeta}_h^+(n) = \frac{1}{b}\int_{-b}^{+b} \zeta_h^+(y)\sin\left[\frac{n\pi}{2b}(y+b)\right]\,\mathrm{d}y, \tag{4.45}$$

are Fourier transforms of the ζ-potentials, which could, in general, depend on x, though such dependence must be 'slow' in the sense of the lubrication approximation. In order to determine the effective ζ-potential, ζ_*, we need $\bar{\psi}$. This may be readily obtained from the above solution for ψ. The calculation may be shortened if we note, that, for separable functions $\psi = \sum A(y)B(z)$, $\bar{\psi} = \sum \overline{A(y)}\,\overline{B(z)}$. We then obtain after some algebra,

$$\bar{\psi} = -\frac{2}{\pi^2}\sum_{n=0}^{\infty}[\mathscr{F}_n(h)\{\tilde{\zeta}_h^+(2n+1) + \tilde{\zeta}_h^-(2n+1)\} + \mathscr{F}_n(h^{-1})\{\tilde{\zeta}_v^+(2n+1) + \tilde{\zeta}_v^-(2n+1)\}], \tag{4.46}$$

where $h = c/b$, the aspect ratio, and $\mathscr{F}$ is a function defined as follows:

$$\mathscr{F}_n(x) = \frac{1}{x}\frac{\tanh[(2n+1)(\pi/2)x]}{(2n+1)^2}. \tag{4.47}$$

The effective ζ-potential, ζ_*, may be evaluated by substituting (4.46), (4.34) and $A = 4bc$ into (4.5) and evaluating the $\langle\ \rangle$ which, in the general case, is best done numerically. In the case of a square cross-section, $h = 1$, it is of interest to note that $\bar{\psi}$ involves only the mean of the Fourier transforms of ζ for each wall. A few special cases of problems with rectangular cross-section are discussed below.

4.2.1. *Flow between parallel plates*

The limit $c/b = h \gg 1$ corresponds to the special case of flow between parallel plates located at $y = \pm b(x)$. Equation (4.33) then reduces to

$$u_p = \tfrac{1}{2}(b^2 - y^2), \tag{4.48}$$

the well-known parabolic profile, so that, $\bar{u}_p = \frac{1}{3}b^2$. Further, on replacing the sinh terms in (4.40) and (4.41) by the linear approximation $\sinh x \approx x$ since the argument of the sinh terms are small, and on noting that the resulting summation over n reduces simply to the Fourier expansion of the ζ-potential, we obtain

$$\psi = \psi_v^+ + \psi_v^- = -\tfrac{1}{2}[\zeta_v^+(x,z) + \zeta_v^-(x,z)] - \frac{y}{2b}[\zeta_v^+(x,z) - \zeta_v^-(x,z)], \tag{4.49}$$

where we have displayed the x-dependence of the ζ-potentials explicitly. The mean over the cross-section, $\bar{\psi}$, may be evaluated from (4.46), but it is easier to simply average (4.49),

$$\bar{\psi} = -\bar{\zeta}(x), \tag{4.50}$$

where

$$\bar{\zeta}(x) = \lim_{c\to\infty} \frac{1}{2c} \int_{-c}^{+c} \tfrac{1}{2} \left[\zeta_v^+(x,z) + \zeta_v^-(x,z)\right] \mathrm{d}z, \tag{4.51}$$

is the average value of the ζ-potential over the boundary of the cross-section. The effective radius, a_*, and ζ-potential, ζ_*, is evaluated easily on substitution of these expressions for $\bar{u}_p$ and $\bar{\psi}$ in (4.4) and (4.5):

$$a_* = (2c)^{1/4} \left[\frac{16}{3\pi\langle 1/b^3\rangle}\right]^{1/4}, \tag{4.52}$$

$$\zeta_* = (2c)^{1/2} \sqrt{\frac{3}{4\pi}} \frac{\langle \bar{\zeta}/b^3\rangle}{\langle 1/b\rangle \langle 1/b^3\rangle^{1/2}}, \tag{4.53}$$

so that (4.6) gives the following expression for the volume flux per unit spanwise length

$$\frac{Q}{2c} = \frac{2}{3} \frac{1}{\langle 1/b^3\rangle} \frac{p_a - p_b}{\mu L} - \frac{\kappa}{4\pi\mu} \frac{2\langle \bar{\zeta}/b^3\rangle}{\langle 1/b\rangle \langle 1/b^3\rangle} \frac{V_a - V_b}{L}. \tag{4.54}$$

In the case where the distance between parallel plates, $2b$, is constant, the above expression for the volume flux reduces to

$$Q = \frac{2b^3}{3\mu} \frac{p_a - p_b}{L} - \frac{\kappa\langle \bar{\zeta}\rangle}{4\pi\mu} \frac{V_a - V_b}{L} (2b). \tag{4.55}$$

That is, for parallel uniformly spaced walls, the volume flux may be calculated simply by replacing the variable ζ-potential by its value averaged over the channel boundaries. This result is exactly analogous to the case of flow through a capillary of uniform radius considered in § 4.1.1 in the lubrication limit, and independently proved earlier by Anderson & Idol for Stokes flow in uniform radius capillaries with ζ-potential varying only in the axial direction.

The phenomenon of electro-osmotic pumping in the absence of a net charge discussed in § 4.1.2 can also be demonstrated using (4.53). Consider a wavy wall

$$b(x) = b_0 + \Delta b \sin\left(\frac{2\pi}{\lambda} x\right), \tag{4.56}$$

together with a sinusoidally varying cross-sectional mean for the ζ-potential

$$\bar{\zeta} = \zeta_0 \sin\left(\frac{2\pi}{\lambda} x + \phi\right). \tag{4.57}$$

The right-hand side of equation (4.54) can easily be evaluated numerically or analytically. In particular, if there is no external pressure head ($p_a = p_b$), and, if $\Delta b \ll b_0$,

$$\frac{q}{2b_0 u_0} = -\frac{3}{2} \frac{\Delta b}{b_0} \cos\phi, \tag{4.58}$$

where $q = Q/(2c)$ is the volume flux per unit span and $u_0 = -(\kappa\zeta_0 E)/(4\pi\mu)$ with $E = (V_a - V_b)/L$ is a characteristic electro-osmotic velocity. Figure 4 shows the dimensionless flow rate $q/(2b_0u_0)$, divided by the amplitude, $\Delta b/b_0$, as a function of the phase ϕ, for several values of $(\Delta b/b_0)$. The symbols indicate the result of direct numerical evaluation from equation (4.54) with $p_a = p_b$, and the single line is the result of using (4.58) valid for $\Delta b/b_0 \ll 1$. Once again, we observe that a mean flow is possible in the absense of a net charge ($\langle\bar{\zeta}\rangle = 0$), as noted by Ajdari. The

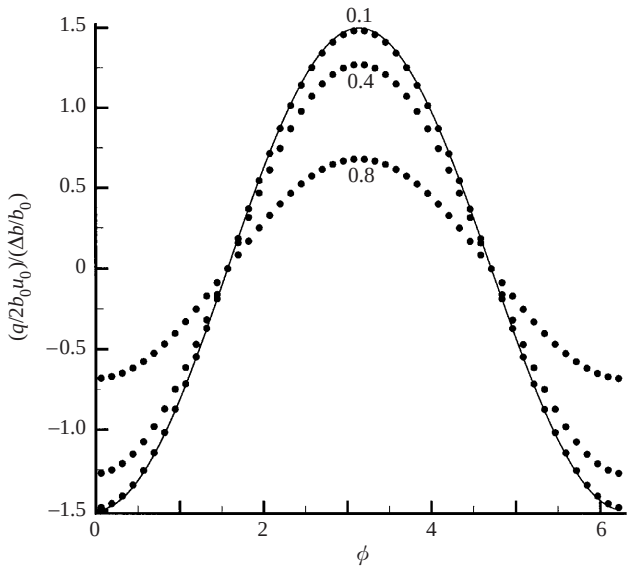

FIGURE 4. The normalized volume flux per unit amplitude as a function of the phase difference ϕ between the wall deformation and ζ-potential for various values of the amplitude, $\Delta b/b_0$, for flow between parallel plates with wavy walls. Symbols indicate the result of using equation (4.54) and the solid line correspond to the small-amplitude approximation to it, equation (4.58).

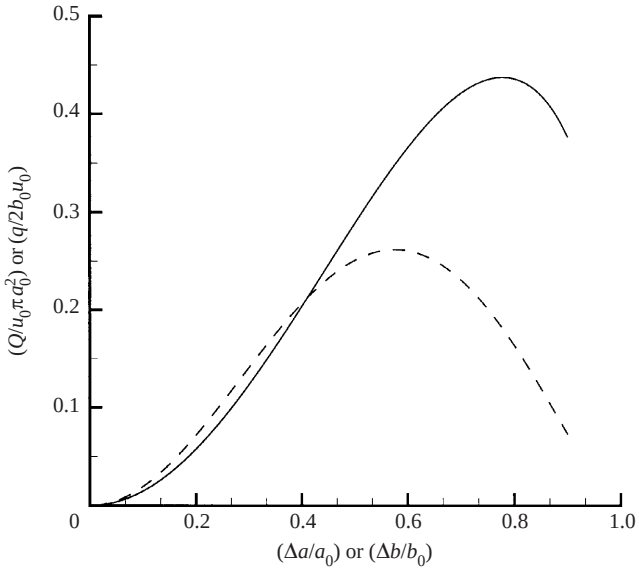

FIGURE 5. The normalized volume flux as a function of the amplitude of deformation in the case of ——, flow between parallel plates, and – – –, through a circular capillary, if the ζ-potential and the wall deformations are exactly out of phase ($\phi = \pi$).

net flow can be in either direction, depending on the phase ϕ. Further, for large deformations of the wall, the flow is no longer linear with respect to the amplitude of deformation, but the magnitude of the flux is smaller than that predicted by the linearized version of (4.54). For a fixed phase ($\phi = \pi$), the flux depends in a nonlinear way on the amplitude $\Delta b/b_0$, as shown in Figure 5. The solid line in figure 5 shows

$(q/2b_0u_0)$ as a function of $\Delta b/b_0$ in the case of parallel walls, the dashed line shows the corresponding quantity $Q/u_0\pi a_0^2$ as a function of $\Delta a/a_0$ in the case of a circular capillary. It can be seen that there exists an optimum deformation for which the flow rate is a maximum.

4.2.2. *Uniformly charged walls*

Microfluidic channels are sometimes made by etching channels on a silicon substrate and then bonding the substrate with a glass plate. In such a situation, the channel is bounded by three silcon surfaces, and one glass surface which has a different ζ-potential. It is therefore of interest to consider the special case when ζ_h^-, ζ_h^+, ζ_v^- and ζ_v^+ are constants, but may not all be equal. In this case, the Fourier transforms of ζ are given by

$$\tilde{\zeta}_h^+(n) = \begin{cases} \dfrac{4\zeta_h^+}{n\pi} & \text{if } n \text{ is odd,} \\ 0 & \text{otherwise,} \end{cases} \tag{4.59}$$

and similarly, for the other three faces. If these expressions are used in (4.46), the result can be written as

$$\bar{\psi} = -\frac{\zeta_v^+ + \zeta_v^-}{2} + (\zeta_v^+ + \zeta_v^- - \zeta_h^+ - \zeta_h^-)\frac{8}{\pi^3}\sum_{n=0}^{\infty}\frac{\mathscr{F}_n(h)}{(2n+1)}, \tag{4.60}$$

where we have used the identity (Gradshteyn & Ryzhik 2000)

$$\sum_{n=0}^{\infty}\frac{1}{(2k+1)^3}[\mathscr{F}_n(x) + \mathscr{F}_n(x^{-1})] = \frac{\pi^3}{16}, \tag{4.61}$$

to eliminate the terms involving $\mathscr{F}_n$. Equation (4.60) shows that the effective ζ-potential is determined by the sum and difference of the average ζ-potential between pairs of opposing walls.

In particular, if all the walls have the same ζ-potential, $\zeta_h^+ = \zeta_h^- = \zeta_v^+ = \zeta_v^- = \zeta_0$, then $\bar{\psi} = -\zeta_0$, a result that is fully expected, since, in this case, $\psi = -\zeta_0$ is the exact solution to the boundary-value problem defining ψ. If three walls have identical ζ-potential, for example $\zeta_h^+ = \zeta_h^- = \zeta_v^- = \zeta_0$ and $\zeta_v^+ = \zeta_1$, then we obtain from (4.60)

$$\bar{\psi} = -\zeta_0 - (\zeta_1 - \zeta_0)\frac{16}{\pi^3}\sum_{n=0}^{\infty}\frac{\mathscr{F}_n(h)}{2n+1}. \tag{4.62}$$

These formulae could be useful in practical applications as they can be used to facilitate the evaluation of (4.4) and (4.5) which enable calculation of the volume flux for arbitrary pressure and potential differences through (4.6).

4.3. *Other cross-sectional shapes*

We have seen that, in the lubrication approximation, the electrohydrodynamic problem of flow through a microchannel reduces to the solution of the pair of boundary-value problems (3.59)–(3.60) and (3.61)–(3.62) defined on a plane, or, equivalently, to the determination of the Green function G for the cross-sectional shape. We have examined two cases, namely microchannels with circular and rectangular cross-sectional shapes, where both these boundary-value problems admit analytical solutions for arbitrary distributions of the ζ-potential. Fortunately, analytical solutions are also obtainable for a variety of other cross-sectional shapes.

Determining ψ involves solving the Laplace equation with Dirichlet boundary conditions, a well-studied problem in mathematical physics, with known solutions for a variety of cross-sectional shapes. The problem (3.59)–(3.60) clearly represents the flow in an infinite cylinder with cross-sectional shape given by the local cross-sectional shape of the microchannel at the location x under a unit pressure gradient. Equations (3.59)–(3.60) also describes the shape of a soap film stretched across a hole, $D(x)$, with an overpressure on one side, a fact exploited by Taylor (1937) to fashion an ingeneous 'analogue computer' for solving (3.59)–(3.60). Finally, the boundary-value problem for u_p is related in a simple way (Love 1944) to the torsion produced in an infinite cylinder whose cross-section corresponds to $D(x)$, when a small twist is applied to it. Analytical solutions for the following domain geometries are known (Love 1944 ch. 14) and could be useful in the context of electro-osmotic flows:

(i) elliptical region,
(ii) sector of a circle,
(iii) curvilinear rectangle bounded by two concentric circular arcs and two radii,
(iv) annular region between two concentric or non-concentric circles,
(v) annular region between two concentric ellipses.

Note, that a trapezoidal domain could be considered to be a special case of (iii), if the radii of the concentric circles become infinitely large, but their difference, and the arc subtended by the radii, remain finite. Trapezoidal shapes are of particular interest, since microfluidic channels made by chemical etching on substrates usually have a trapezoidal cross-section.

5. Conclusion

The problem of electro-osmotic flow in a straight microfluidic channel was considered in situations where the wall ζ-potential and cross-sectional shape could vary in the axial direction. Such non-uniformities in the ζ-potential could arise by accident or by design. The pressures and voltages at the inlet and outlet sections of the channel are considered known. The problem was formulated in the limit where the Debye layer thickness at the wall is negligible in comparison to a characteristic channel width, so that the coupling between the electrostatic and hydrodynamic problems could be described through the Helmholtz–Smoluchowski slip boundary conditions.

Since microfluidic channels are usually of macroscopic size in the axial direction though the characteristic width is measured in micrometres, for a wide range of practical problems it may be a good approximation to consider the characteristic width to be very much smaller than the characteristic length scale for axial variation in channel properties (cross-sectional area, shape and wall ζ-potential). In the limit when the ratio of these two scales is small (the lubrication limit), it was shown that the electrohydrodynamic problem admits a simple solution, the evaluation of which requires only a knowledge of the Green function for the Laplace operator with zero boundary conditions corresponding to each cross-section of the channel. Thus, in situations where the Green function, or equivalently, the functions u_p and ψ related to it, can be determined analytically, the problem of electro-osmotic flow admits an analytical solution. Even in situations where the Green function cannot be determined analytically, the numerical problem of determining the flow is reduced to solving a sequence of two-dimensional linear problems, a much simpler task than integrating the full three-dimensional Navier–Stokes or Stokes equations.

One of the consequences of the lubrication solution is that the flow rate through any section of a straight microfluidic channel with variable axial properties is the same as

that through a uniform cylindrical capillary with a certain 'equivalent' radius a_* and ζ-potential, ζ_*, that is determined solely by the geometry and wall charge distribution in the channel. In the special case of a cylindrical capillary, ζ_* reduces simply to the axially averaged value of ζ in agreement with an earlier result due to Anderson & Idol. In electrical circuit analysis, various components in a branch of a circuit may be lumped into a single complex number (the electrical impedance) for the purpose of calculation of the currents through various branches of the network. The equivalent radius and ζ-potential could similarly be used to characterize the resistance to fluid flow in each branch of a microfluidic circuit on application of any combination of external pressure head and electrical voltage. Such 'circuit analysis' ideas have already been applied to simple microfluidic junctions (Jacobson, McKnight & Ramsey 1999).

A common difficulty in capillary electrophoresis of proteins is the tendency of the analyte to stick to the walls of the channel (Towns & Regnier 1991). This, in turn, affects both the bulk flow and the velocity profile across the channel cross-section owing to the appearance of an induced pressure gradient that must result in order to satisfy the requirement of continuity. The lubrication approximation allows us to calculate this pressure gradient and the associated modification of the velocity field for any known ζ-potential distribution. However, in the problem of electrophoresis in the presence of adsorbing walls, this distribution itself evolves in time in a way determined by the adsorption properties of the wall, diffusive properties of the analyte and the flow field itself. The full problem of axial dispersion of an analyte in an adsorbing channel driven by an electro-osmotic flow is difficult and has not been addressed analytically, though some numerical simulations of the underlying equations have been reported (Ermakov *et al.* 1995; Potoček *et al.* 1995; Schure & Lenhoff 1993; Zhukov, Ermakov & Righetti 1997). The lubrication analysis presented here, could be useful as a component of such a theoretical analysis that may be developed. Analytical solutions have been obtained recently for reduced versions of the full problem in two special cases. In the first case, travel time for a plug of adsobing analyte across a fixed length of capillary was calculated by assuming an *ad hoc* functional form for the modified ζ-potential behind the plug (Ghosal 2002*a*). In the second case, Taylor dispersion of a non-adsorbing analyte in a cylindrical capillary, a section of which is coated to alter the wall ζ-potential was calculated (Ghosal 2002*b*). In either case, good agreement with experiments are obtained. The lubrication theory presented here could serve as a starting point for a complete analytical theory of Taylor dispersion in capillaries with adsorbing walls in general geometries. Some progress in this direction has been made, and will be reported on in a future paper.

Another result that follows readily from our expression for the effective ζ-potential is that a net fluid flux may develop in a channel in the absence of an external pressure head, even if the total charge on the walls is zero (that is $\langle\bar{\zeta}\rangle = 0$). This is because ζ_* involves a weighted average of the local ζ-potential with a weight determined by quantities related to the channel geometry. Therefore, $\langle\bar{\zeta}\rangle = 0$ implies $\zeta_* = 0$, only if the geometry of the channel cross-section does not change in the axial direction. The possibility of a net flow in the absence of a net charge was noted by Ajdari, who showed it in the special case of flow between two parallel walls, one of which has small sinusoidal variations in ζ-potential and the other has small sinusoidal deformations on its surface. The lubrication analysis shows this effect in a more general context for channels of arbitrary cross-section and wall charge distributions. In particular, for a cylindrical capillary and flow between parallel plates, the flow rate is explicitly calculated, and its dependence on the amplitude and relative phase of the perturbations in channel shape and wall charge is shown.

The lubrication analysis reduces the problem of electro-osmotic flow to determining the Green function G for any cross-section, or equivalently, solving two boundary-value problems for the quantities ψ and u_p. The function ψ is defined by a two-dimensional Laplace equation with Dirichlet boundary conditions, and u_p is defined by a Poisson's equation with zero boundary conditions. Explicit analytical solutions for u_p and ψ are presented for channels of circular and rectangular cross-sections. In the special case of a uniform circular cylinder with no imposed pressure head and a wall ζ-potential that varies sinusoidally in the axial direction, an analytical solution is obtained and compared with the exact solution to the corresponding Stokes flow problem. The two solutions are found to be in excellent agreement if the ratio of channel radius (a_0) to wavelength (λ) of the ζ-potential perturbation is less than 0.1. The asymptotic solution differs significantly from the exact solution in the 'opposite' limit $a_0/\lambda \gg 1$. For $a_0/\lambda > 10$, the character of the flow changes qualitatively and may no longer be described by the lubrication solution. In this regime, the flow in the bulk of the channel does not 'see' the fluctuations in the ζ-potential and develops a 'pure' electro-osmotic flow driven by the mean ζ-potential. The effect of the rapid fluctuations is felt in a narrow boundary layer where a region of high shear exists. Finally, it should be noted that neither the lubrication solution nor the exact solution takes account of inertial effects. In the lubrication limit, the inertial terms are of order $(a_0/\lambda)Re$ (where Re is a Reynolds number based on channel radius and characteristic electro-osmotic velocity) and do not appear at leading order even if $Re \sim 1$. In the analytical solution of Anderson & Idol, it is assumed that Re is negligible so that the solution for the Stokes equation is exact.

The lubrication analysis presented here could provide a starting point for various other problems in the electro-osmotic flow in channels of general geometry. In particular, the solution for the axial velocity could be used in the analysis of Taylor dispersion of scalars in microfluidic channels due to axial variations in wall properties. This is a problem of great importance in microfluidics since 'band spreading' due to Taylor dispersion limits the resolution of electrophoretic separations.

The author wishes to thank Professors Joseph B. Keller and Howard Stone for their helpful comments on this work, and anonymous referees for bringing several relevant references to the author's attention.

REFERENCES

Abramowitz, M. & Stegun, I. A. (Eds.) 1970 *Handbook of Mathematical Functions.* Dover.

Ajdari, A. 1995 Electro-osmosis on inhomogeneously charged surfaces. *Phys. Rev. Lett.* **75**, 755–758.

Ajdari, A. 1996 Generation of transverse fluid currents and forces by an electric field: Electro-osmosis on charge-modulated and undulated surfaces. *Phys. Rev.* E **53**, 4996–5005.

Anderson, J. R., Chiu, D. T., Jackman, R. J., Cherniavskaya, O., McDonald, J. C., Wu, H., Whitesides, S. H. & Whitesides, G. M. 2000 Fabrication of topologically complex three-dimensional microfluidic systems in PDMS by rapid prototyping. *Anal. Chem.* **72**, 3158–3164.

Anderson, J. L. & Idol, W. K. 1985 Electroosmosis through pores with nonuniformly charged walls. *Chem. Engng Commun.* **38**, 93–106.

Anderson, J. R., McDonald, J. C., Stone, H. A. & Whitesides, G. M. 2001 Integrated components in microfluidic devices in PDMS: a biomimetic check valve, pressure sensor and reciprocating pump. Preprint.

Barkar, S. L. R., Ross, D., Tarlov, M. J., Gaitan, M. & Locascio, L. E. 2000 Control of flow direction in microfluidic devices with polyelectrolyte multilayers. *Anal. Chem.* **72**, 5925–5929.

Batchelor, G. 1967 *An Introduction to Fluid Dynamics.* Cambridge University Press.

Berry, R. M. 1993 Torque and switching in the bacterial flagellar motor: an electrostatic model. *Biophys. J.* **64**, 961–973.

Culbertson, C. T., Jacobson, S. C. & Ramsey, J. M. 1998 Dispersion sources for compact geometries on microchips. *Anal. Chem.* **70**, 3781–3789.

Day, R. F. & Stone, H. A. 2000 Lubrication analysis and boundary integral simulations of a viscous micropump. *J. Fluid Mech.* **416**, 197–216.

Ermakov, S. V., Zhukov, M. Y., Capelli, L. & Righetti, P. G. 1995 Wall adsorption in capillary electrophoresis, experimental study and computer simulation. *J. Chromatog.* A **699**, 297–313.

Ghosal, S. 2002*a* Effect of analyte adsorption on the electroosmotic flow in microfluidic channels. *Anal. Chem.* **74**, 771–775.

Ghosal, S. 2002*b* Does Taylor dispersion induced by flow modification explain band broadening in a partially coated microcapillary? Preprint.

Gradshteyn, I. S. & Ryzhik, I. M. 2000 *Table of Integrals, Series and Products.* Academic.

Hayes, M. A. & Ewing, A. G. 1992 Electroosmotic flow control and monitoring with an applied radial voltage for capillary zone electrophoresis. *Anal. Chem.* **64**, 512–516.

Herr, A. E., Molho, J. I., Santiago, J. G., Mungal, M. G. & Keny, T. W. 2000 Electroosmotic capillary flow with nonuniform zeta potential. *Anal. Chem.* **72**, 1053–1057.

Jacobson, S. C., McKnight, T. E. & Ramsey, J. M. 1999 Microfluidic devices for electrokinetically driven parallel and serial mixing. *Anal. Chem.* **71**, 4455–4459.

Jakeway, S. C., de Mello, A. J. & Russell, E. L. 2000 Miniaturized total analysis systems for biological analysis. *Fresen. J. Anal. Chem.* **366**, 525–539.

Lambert, W. J. & Middleton, D. L. 1990 pH hysterisis effect with silica capillaries in capillary zone electrophoresis. *Anal. Chem.* **62**, 1585–1587.

Lammert, P. E., Prost, J. & Bruinsma, R. 1996 Ion drive for vescicles and cells. *J. Theor. Biol.* **178**, 387–391.

Lee, C. S., Blanchard, W. C. & Wu, C. 1990 Direct control of the electroosmosis in capillary zone electrophoresis by using an external electric field. *Anal. Chem.* **62**, 1550–1552.

Lighthill, M. J. 1968 Pressure-forcing of tightly fitting pellets along fluid-filled elastic tubes. *J. Fluid Mech.* **34**, 113–143.

Liu, Y., Fanguy, J. C., Bledsoe, J. M. & Henry, C. S. 2000 Dynamic coating using polyelectrolyte multilayers for chemical control of electroosmotic flow in capillary electrophoresis microchips. *Anal. Chem.* **72**, 5939–5944.

Long, D., Stone, H. A. & Ajdari, A. 1999 Electroosmotic flows created by surface defects in capillary electrophoresis. *J. Colloid Interface Sci.* **212**, 338–349.

Love, A. E. H. 1944 *A Treatise on the Mathematical Theory of Elasticity*. Dover.

Patankar, N. A. & Hu, H. H. 1998 Numerical simulation of electroosmotic flow. *Anal. Chem.* **70**, 1870–1881.

Potoček, B., Gaš, B., Kenndler, E. & Štědrý, M. 1995 Electroosmosis in capillary zone electrophoresis with nonuniform zeta potential. *J. Chromatog.* A **709**, 51–62.

Probstein, R. 1994 *Physicochemical Hydrodynamics.* John Wiley.

Reuss, F. F. 1809 Sur un nouvel effet de l'électricitè galvanique. *Mémoires de la Societé Impériale des Naturalistes de Moscou* **2**, 327–337.

Schure, M. R. & Lenhoff, A. M. 1993 Consequences of wall adsorption in capillary electrophoresis: theory and simulation. *Anal. Chem.* **65**, 3024–3037.

Secomb, T. W., Skalak, R., Özkaya, N. & Gross, J. F. 1986 Flow of axisymmetric red blood cells in narrow capillaries. *J. Fluid Mech.* **163**, 405–423.

Stroock, A. D., Weck, M., Chiu, D. T., Huck, W. T. S., Kenis, P. J. A., Ismagilov, R. F. & Whitesides, G. M. 2000 Patterning electro-osmotic flow with patterned surface charge. *Phys. Rev. Lett.* **84**, 3314–3317.

Taylor, G. I. 1937 The determination of stresses by means of soap films. In *The Mechanical Properties of Fluids (a collective work).* Blackie.

Towns, J. K. & Regnier, F. E. 1991 Capillary electrophoretic separations of proteins using nonionic surfactant coatings. *Anal. Chem.* **91**, 1126–1132.

Towns, J. K. & Regnier, F. E. 1992 Impact of polycation adsorption on efficiency and electro-osmotically driven transport in capillary electrophoresis. *Anal. Chem.* **64**, 2473–2478.

Whitesides, G. M. & Stroock, A. D. 2000 Flexible methods for microfluidics. *Phys. Today* **54**, 42–48.

Whitham, G. B. 1963 The Navier–Stokes equations of motion. In *Laminar Boundary Layers* (ed. L. Rosenhead). Oxford University Press.

Zhukov, M. Y., Ermakov, S. V. & Righetti, P. G. 1997 Simplified mathematical model of irreversible sample adsorption in capillary zone electrophoresis. *J. Chromatog.* A **766**, 171–185.